Research Article

Xin Meng, Xiaoyu Jia, Yuanzhang Qi, Dagang Miao, and Xu Yan*

Fabrication of polylactic acid nanofibrous yarns for piezoelectric fabrics

https://doi.org/10.1515/epoly-2023-0030
received April 06, 2023; accepted April 26, 2023

Abstract: With the rapid development of smart wearable devices and the urgent demands for new energy resources, fibrous flexible power supply units had attracted a lot of interest. Here, we reported the fabrication of polylactic acid (PLA) piezoelectric nanofibrous yarn-based fabric through conjugated electrospinning and weaving process. Five kinds of PLA yarns including poly(L-lactide) (PLLA), poly(D-lactide) (PDLA), PLLA positive/PDLA negative, PDLA positive/PLLA negative, and PLLA/PDLA mixture (1:1 w/w) ones were prepared and investigated. Among these, the PLLA/PDLA yarn had more uniform and oriented structure with 301 MPa tensile strength, which could meet the requirement of weaving. A 4 cm × 4 cm woven PLLA/PDLA fabric could provide a maximum current of 90.86 nA and a voltage of 8.69 V under 5 N force, and the piezoelectricity could be enhanced by the fabric area and the applied force. This approach may be helpful for the design of wearing generators.

Keywords: polylactic acid, conjugated electrospinning, nanofiber yarns, fabric, piezoelectricity

*** Corresponding author: Xu Yan,** Industrial Research Institute of Nonwovens and Technical Textiles, Shandong Center for Engineered Nonwovens, College of Textiles and Clothing, Qingdao University, Qingdao 266071, China; State Key Laboratory of Bio-Fibers and Eco-Textiles, Qingdao University, Qingdao 266071, China, e-mail: yanxu-925@163.com
Xin Meng, Xiaoyu Jia: Industrial Research Institute of Nonwovens and Technical Textiles, Shandong Center for Engineered Nonwovens, College of Textiles and Clothing, Qingdao University, Qingdao 266071, China
Yuanzhang Qi: Lufeng Company Co., Ltd., Zibo 255100, China
Dagang Miao: Industrial Research Institute of Nonwovens and Technical Textiles, Shandong Center for Engineered Nonwovens, College of Textiles and Clothing, Qingdao University, Qingdao 266071, China; State Key Laboratory of Bio-Fibers and Eco-Textiles, Qingdao University, Qingdao 266071, China

1 Introduction

Nowadays, under the background of carbon neutralization, the development of renewable and environmentally friendly energy technologies was urgently needed to replace the traditional fossil energy (1–8). In addition to the rapid development of intelligent wearable technology, light and wearable power supply units were also a urgent demand (9–11).

Recently, various materials were developed to collect energy based on different working mechanisms, such as piezoelectricity (12–14) and triboelectricity (15,16). Specifically, piezoelectric nanogenerators (PENGs) which convert mechanical energy into electrical energy through piezoelectric materials had attracted a lot of interest since 2006 (13). Piezoelectric materials were expanded from inorganic materials such as ZnO (13), $BaTiO_3$ (17), and perovskite lead zirconate titanate (18) to polymers including poly(vinylidene fluoride) (PVDF) (19), poly(lactide) (PLA) (20), and their copolymers. To obtain flexible PENGs for wearing, these materials had been isolated or blended electrospun into nanofibrous films (21–23). Among these electrospun piezoelectric films, the PLA-based ones had been paid much attention due to its low cost, biodegradability, and biocompatibility (24,25). Generally, PLA had two isomers, namely poly(L-lactide) (PLLA) and poly(D-lactide) (PDLA) (26). Both PLLA and PDLA exhibited weak piezoelectricity (27,28). It had been reported that the PDLA/PLLA multilayer films could generate a larger piezoelectric resonance (28–30).

However, the flexible piezoelectric films still had some shortcomings in wearable applications, such as poor air permeability and being less comfortable to wear (31). To overcome these challenges, various self-powered yarns and fabrics were developed (32–34). Dai et al. had prepared poly(vinylidene fluoride-co-tri-fluoroethylene) P(VDF-TrFE) piezoelectric yarns by electrospinning, and the woven fabrics achieved 38 nA current and 2.7 V voltage under 15 N pressure (32). However, PLA nanofibrous yarns were rarely mentioned in that study.

In this article, we reported the fabrication of PLA yarns by conjugated electrospinning, which had two

spinnerets with opposite polarity. Here, five types of PLA yarns were prepared including pure PLLA yarn, pure PDLA yarn, PLLA positive/PDLA negative yarn, PLLA negative/PDLA positive yarn, and PDLA/PLLA yarn. The morphology of the prepared yarns was examined by scanning electron microscope (SEM). The crystalline properties and mechanical properties of the yarns were also investigated. The yarns were woven into fabrics, and the piezoelectric properties of the fabrics were examined.

2 Materials and methods

2.1 Materials

PLLA (Dongguan Wanda Plastic Raw Materials Co., Ltd, 4032D), PDLA (Dongguan Wanda Plastic Raw Materials Co., Ltd, 4043D), and the mixture of PLLA and PDLA (1:1 w/w) were dissolved into *N*,*N*-dimethylformamide (Shanghai Sinopharm Chemical Reagent) at ambient temperature, humidity, and stirring for 24 h at room temperature. The PLLA, PDLA, and the PLLA/PDLA solution concentrations were all 8 wt%. A copper wire with a diameter of 0.05 mm (B&R Company, China) was selected as the core yarn and conductive electrode.

2.2 Preparation of continuous PLA nanofiber yarns and fabric

The conjugate electrospinning process is illustrated in Figure 1. Before electrospinning, the prepared solution was loaded into a 5 mL nozzle with a 25-gauge flat metal nozzle and placed in the nozzle holder of the conjugate spinning machine, using the Cu fiber as the core electrode, and the spinning parameters were set as follows: the distance between the nozzle and the trumpet collector of 12 cm, the positive and negative voltage of ±6.5 kV, the solution feeding rate of 0.4 mL·h^{-1}, the yarn winding speed rate of 1 mm·min^{-1}, and the speed of the trumpet of 300 rpm.

During the electrospinning process, the positive and negative high-voltage power supply connected to the two spinnerets and the positive- and negative-charged jets were spayed and flied onto the trumpet to form a fiber bundle (32,34), as suggested in Figure 1a and b. Here, we chose five combinations of spinning solutions connected to the positive/negative power supply, which were pure PLLA, pure PDLA, PLLA positive/PDLA negative, PDLA positive/PLLA negative, and PLLA/PDLA mixture. With the rotating of the trumpet, the as-spun fibers were twisted onto the core Cu wire (Figure 1c) and then the continuous core-spun PLA/Cu yarns were obtained, as

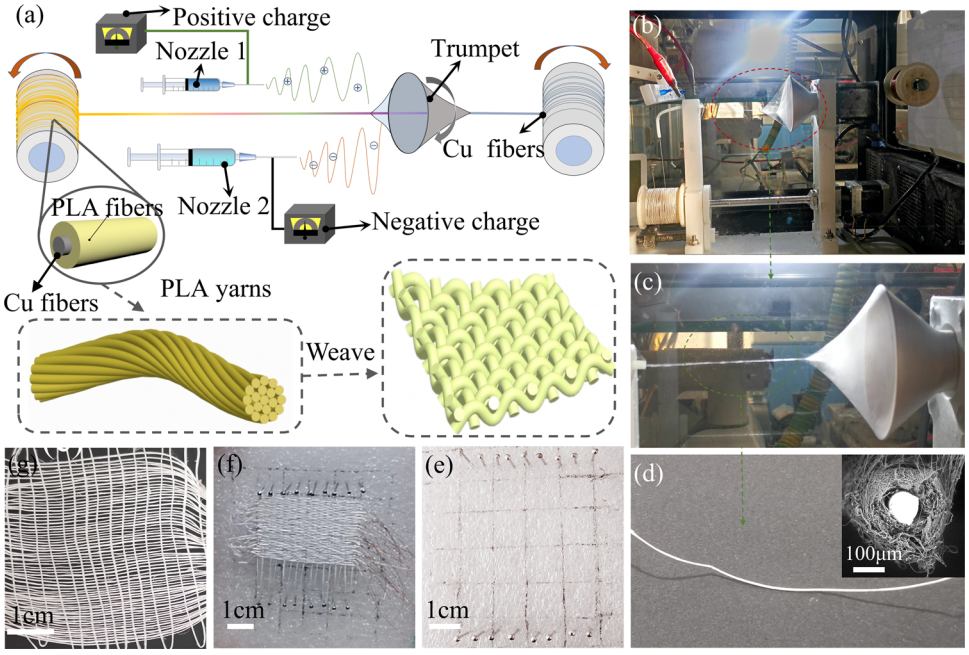

Figure 1: Preparation process of conjugated electrospun PLA nanofiber yarns and fabrics: (a) schematic diagram of conjugated electrospun Cu core/PLA shell yarn, (b) devices for conjugated electrospun PLA nanofiber yarn, (c) the twisting trumpet during electrospinning process, (d) the obtained PLA nanofiber yarn and the cross section images of the yarn, (e) home-made weaving device, (f) hand-weaving process, and (g) the prepared PLA fabric.

shown in Figure 1d. Through a small home-made spinning device shown in Figure 1e, the continuous flexible PLA nanofiber yarns were woven into 1/1 plain fabric with warp and weft yarns of the same type. Moreover, during the hand-weaving process as suggested in Figure 1f, the warp yarn density was 17 cm^{-1} and the weft yarn density was 4 cm^{-1}. The obtained fabric is displayed in Figure 1g.

2.3 Characterization

The real images of the prepared yarns and fabrics were taken using a mobile phone camera (Huawei, Honor 20). The morphology of the prepared nanofiber yarns was observed by a desktop SEM (Phenom Pro, Thermo Fisher Scientific). The crystalline melting behavior of the prepared PLA fibers was examined by a differential scanning calorimeter (DSC, Mettler Toledo, Switzerland) under the protection of nitrogen and at a room temperature of 23–250°C with a ramp-up rate of 10°C·min^{-1}. The chemical structures of the as-spun PLA fibers were characterized by infrared spectroscopy (Nicolet 5700; Thermo Fisher Scientific, USA) in the range of 500–4,000 cm^{-1}. The mechanical properties of the yarns and fabrics were tested by a universal tensile strength machine (Instron 3382, Instron, USA) with a length of 70 mm and a 4 cm × 4 cm area at a stretching speed of 10 mm·min^{-1}, respectively.

The PLA fabric samples were completely wrapped with polyimide tape, and the twisted Cu cores of the warp yarns were used as the electrode. The piezoelectricity of the fabric was examined by a laboratory-assembled piezoelectric test equipment with a picoammeter (Keithley 6487), current amplifier (SR570), and digital oscilloscope (GDS-2102; GW Instek). The pressure was provided by a circulation device (ds-400) with a reciprocating telescopic linear speed regulator and checked by a tensimeter (HG-100; HBO instrument, China).

3 Results and discussion

3.1 Morphology of the prepared PLA nanofiber yarns

Figure 2 shows the morphology of the prepared PLA as-spun yarns and fibers with different combinations, including pure PLLA yarn (Figure 2a and a1), pure PDLA yarn (Figure 2b and b1), PLLA/PDLA yarn (Figure 2c and c1), PLLA positive/PDLA negative (Figure 2d and d1), and PDLA

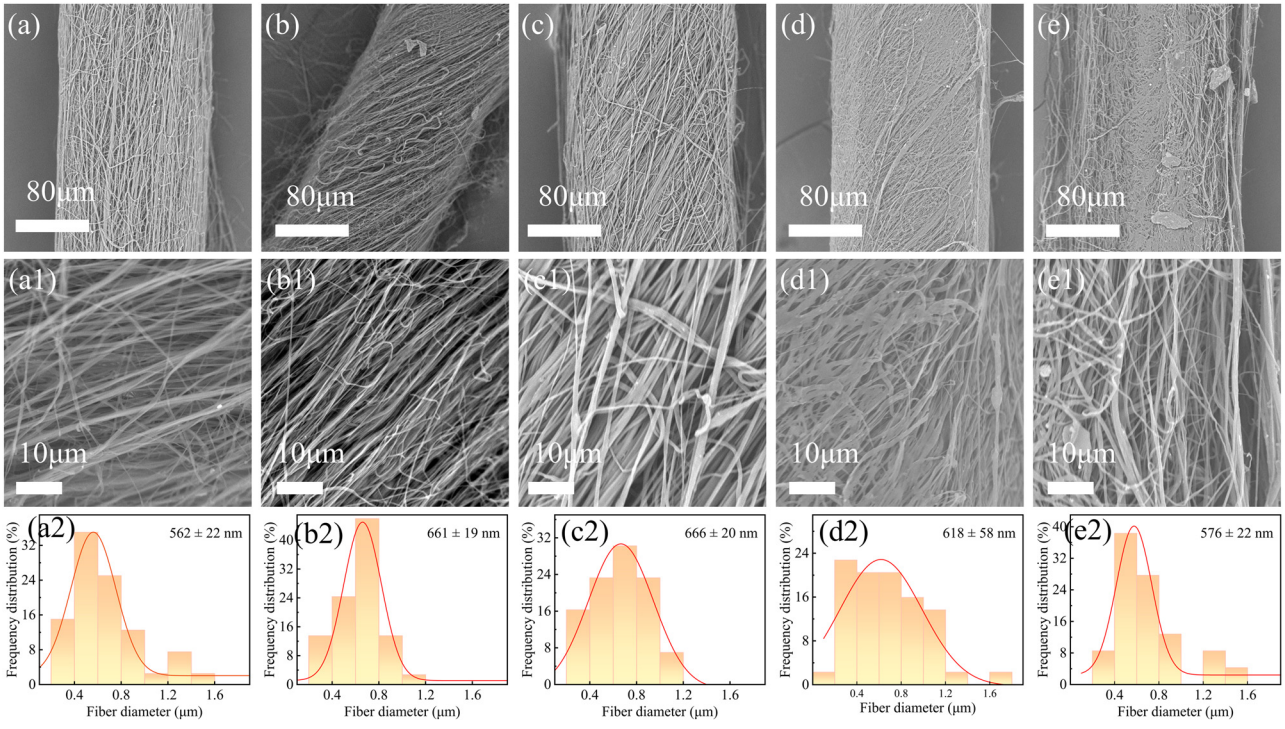

Figure 2: SEM images of as-spun PLA yarns and fibers. (a) PLLA yarn, (b) PDLA yarn, (c) PLLA/PDLA yarn, (d) PLLA positive/PDLA negative yarn, (e) PDLA positive/PLLA negative yarn, and the SEM images of corresponding fibers (a1–e1), as well as the fiber diameter distribution (a2–e2).

positive/PLLA negative (Figure 2e and e1). It could be found that in each case, the electrospun PLA fibers twined round the Cu core tightly forming a relatively uniform covering yarn without any obvious nodules and defects. The surface fibers of the yarns generally had a directional arrangement due to the twisting process.

Moreover, from Figure 2a1–e1, it was found that when the positive and negative power supply connected to the same solution (Figure 2a1–c1), the as-spun fibers were more smooth, uniform, and better oriented than the different solution cases (Figure 2d1 and e1). This may be due to the following reasons: the uneven charge distribution in the different solution jets, the as-spun fibers with larger difference in diameter being interspersed with each other, and the adhesion phenomenon would have affected the fibers' morphology.

The distribution of the fiber diameters is shown in Figure 2a2–e2. It could be found that the electrospun pure PLLA fibers had smaller diameters of about 562 ± 22 nm (Figure 2a2), and the as-spun pure PDLA fibers had average diameters of about 661 ± 19 nm (Figure 2b2). However, when the PLLA and PDLA were mixed in the solution, the as-spun fibers had a larger average diameter of about 666 ± 20 nm (Figure 2c2). When the PLLA and PDLA were electrospun with different power polarity, the average fiber diameters were located in the range of pure PLLA and PDLA ones.

3.2 FTIR and DSC analysis of electrospun PLA fibers

Figure 3 shows the fourier transform infrared (FTIR) spectra and DSC curves of the PLA raw materials and the as-spun PLA fibers. From the FTIR spectra in Figure 3a, we found that the characteristic absorption peaks of all PLA species were almost the same, with C–H stretching vibration absorption peaks at around 3,002–2,932 cm^{-1} and C═H stretching vibration absorption peaks at 1,750 cm^{-1}, bending vibration absorption peaks of C–H of $–CH_3$ at 1,452 cm^{-1}, 1,380 cm^{-1}, C═H bending vibration absorption peaks at 1,180 cm^{-1}, and the asymmetric stretching and symmetric stretching vibrational peaks of C–O–C at 1,085 cm^{-1}. This suggested that none of the characteristic peaks of the various PLA was changed after electrospinning.

Figure 3b displays the DSC results for different types of electrospun PLA nanofibers (PLLA, PDLA, PDLA/PLLA). It was suggested that with the increase of temperature, all PLA fibers showed an exothermic peak at around 70°C. When the temperature raised to more than 150°C, melt peaks appeared in the pure PLLA, pure PDLA, PLLA positive/PDLA negative, and PLLA negative/PDLA positive samples. For pure PLLA electrospun fiber, there were two higher peaks, and PDLA fiber had one peak; both the PLLA positive/PDLA negative and PLLA negative/PDLA positive fibers also had two weaker peaks due to the mixture of PLLA and PDLA fibers (28,30). However, for the electrospun PDLA/PLLA (1:1 w/w) fibers, the melting point shifted to approximately 220°C with a melting point increase of approximately 50°C and better heat resistance (35,36), which might result from the formation of stereocomplex crystal in the mixture of PDLA and PLLA (26,35,36).

3.3 Mechanical properties of PLA yarns and fabrics

The mechanical properties of the as-spun PLA yarns were first investigated to ensure that they could meet the

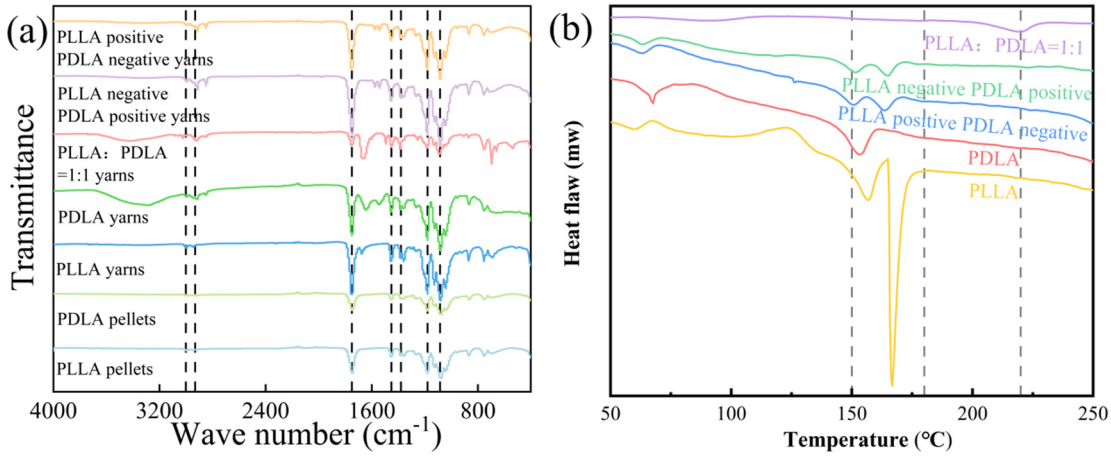

Figure 3: (a) FTIR spectra of PLLA, PDLA powders, and the different types of electrospun PLA fibers and (b) DSC curves of the as-spun PLA fibers.

weaving requirements. As shown in Figure 4a, the crystallinity of the samples affected its tensile properties, so there was a large difference in mechanical properties between the different types of PLA yarns. The semi-crystalline pure PLLA yarn had a tensile strain of 16.2% and a tensile strength of 265 MPa, which were much less than the crystalline pure PDLA yarn with a tensile strain of 23.2% and a tensile strength of 285 MPa; the yarn formed by spinning PLLA and PDLA at different polarity charges had the expected tensile strain and strength between PLLA and PDLA. Remarkably, the tensile strain of the PLLA/PDLA yarns was 24.9% and the tensile strength was 301 MPa, which were consistent with the previously assumed results. These results suggested that the PLLA/PDLA yarn could meet the requirements for weaving.

By home-made weaving tools, the prepared PLA yarns were woven into fabrics, as displayed in Figure 4b. The mechanical properties of the fabrics were also examined and shown in Figure 4c. Similar to the PLA yarns, the PLLA/PDLA fabric had the highest tensile strength. Obviously, the stress–strain curves of the fabric were not straight lines but a stepwise variation. The reason was that the yarns in the fabric did not break in the ideal way (all yarns break at the same time), but partly and in sequence. Therefore, the stretching device did not stop immediately at the start of breaking, but continued to stretch until the stress dropped by 30% before defaulting to complete breaking. These test results proved that the prepared PLLA/PDLA fabrics had excellent mechanical properties for wearing.

Nowadays, the wearing power supply required flexibility to adapt to various use environments. As shown in Figure 4d, the flexibility of the prepared fabrics was examined by bending, deformation, and restoration. It was found that the PLLA/PDLA fabric could be bent over 180° and even after applying strong external forces, it could recover fast from deformation with structural stability. The flexibility and stability of the PLLA/PDLA fabric ensured it could be potentially applied for wearing.

3.4 Piezoelectric properties of flexible PLA fabrics

It had been reported that electrospun PLA could enhance orientation and result piezoelectricity under the polarizing effect of the external electric field (27). Accordingly, we examined the piezoelectric properties of the prepared fabrics. First, the piezoelectric voltages of the different PLA fabrics suggested in Figure 4b were tested. As shown in Figure 5a and b, all the prepared PLA fabrics showed

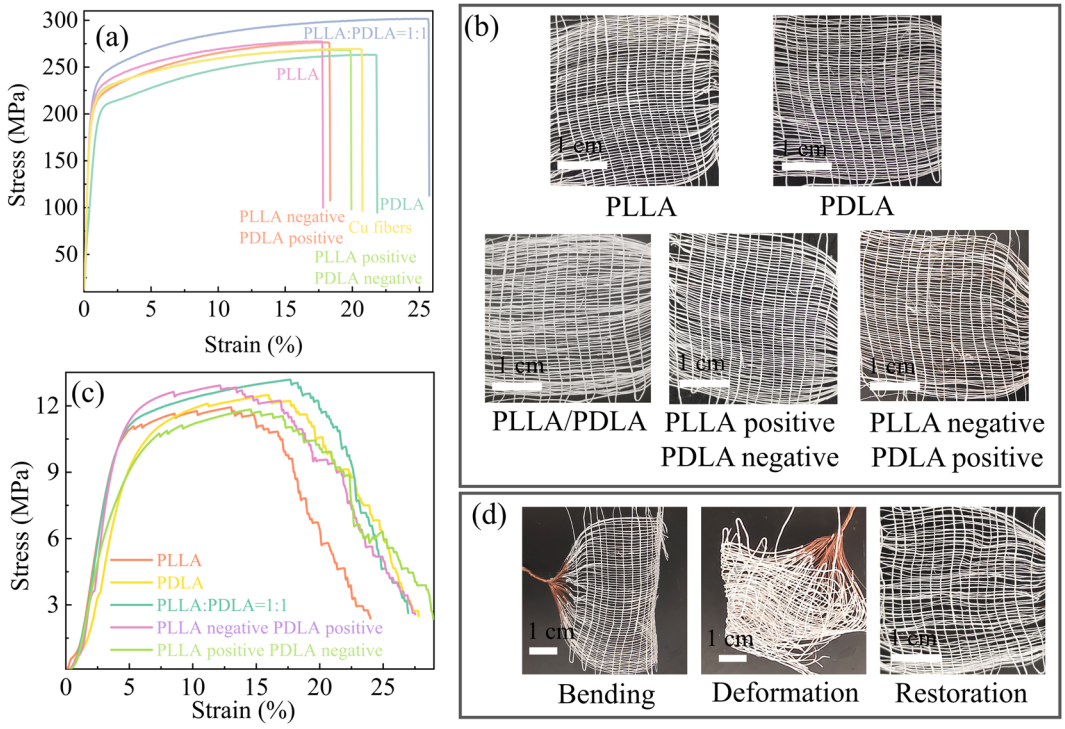

Figure 4: (a) Stress–strain curves of the as-spun PLA yarns, (b) the prepared PLA fabrics of 4 cm × 4 cm with different PLA yarns, (c) stress–strain curves of the PLA fabrics, and (d) the flexibility of the PLLA/PDLA fabrics.

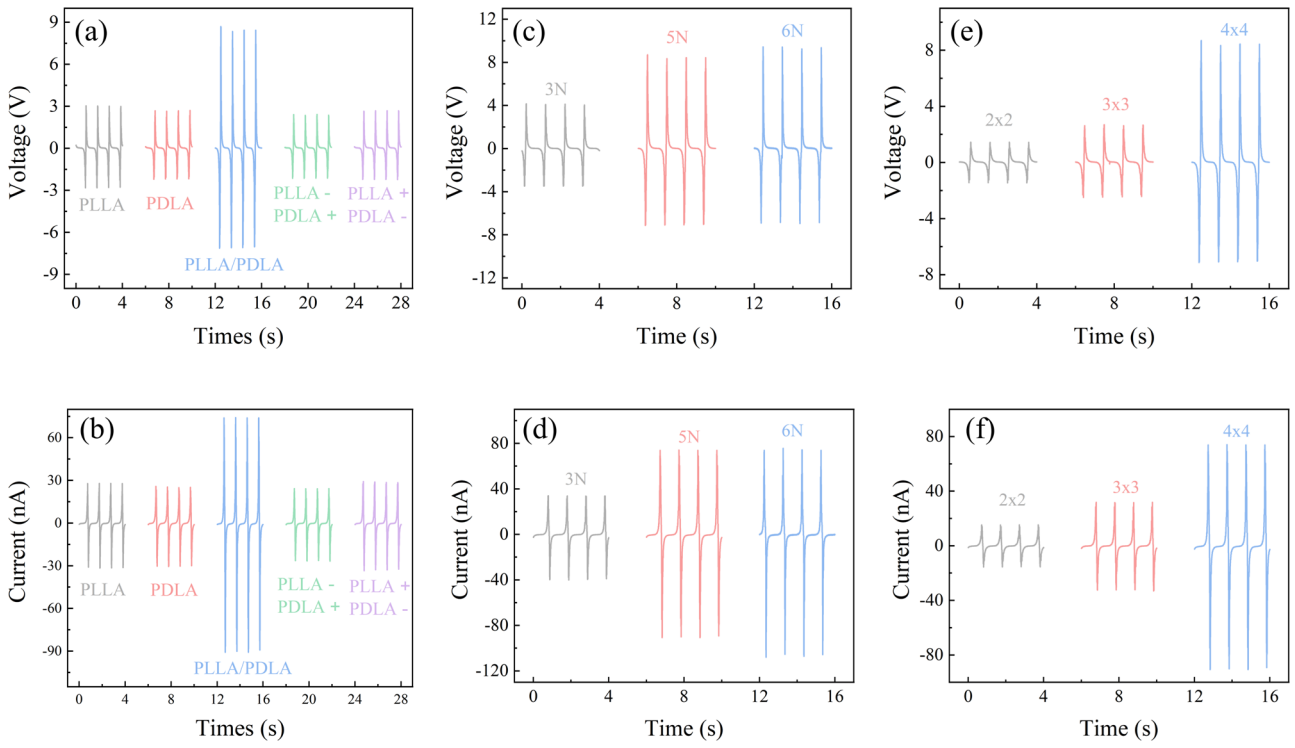

Figure 5: The piezoelectric voltages (a) and currents (b) of 4 cm × 4 cm PLA fabrics under 5 N forces, the voltages (c) and currents (d) of 4 cm × 4 cm PLLA/PDLA fabric under different forces, and the voltages (e) and currents (f) of PLLA/PDLA fabric with different areas under 5 N forces.

piezoelectricity under 5 N forces, and the PLLA/PDLA fabric had the highest open circuit charge of 8.69 V and a short circuit current of 90.86 nA (Figure 5b), which were higher than the PVDF nanofibrous fabric (32). Compared with the pure PLLA fabric, the generated voltage and current increased about 228% and 210%, respectively. The increasing of the piezoelectricity of the PLLA/PDLA one may be attributed to the forming of a stereocomplex crystal in the mixture of PDLA and PLLA, as suggested in Figure 3b.

Moreover, the piezoelectric properties of the PLLA/PDLA fabrics were examined under different forces and different areas, as displayed in Figure 5c–f. It was found that with the increasing forces and areas, the generated voltages and currents were also improved. These results indicated that the prepared PLLA/PDLA nanofibrous fabric had potential application in flexible power supply for wearing.

4 Conclusions

In summary, we had successfully prepared various PLA nanofibrous yarns by conjugate electrospinning. Since the conjugate electrospinning contained two spinnerets connected to opposite polarity power supply, we designed five types of PLA nanofibrous yarns including pure PLLA, pure PDLA, PLLA positive/PDLA negative, PDLA positive/PLLA negative, and PLLA/PDLA mixture (1:1 w/w) ones. It was found that the two spinnerets with the same solutions would produce more uniform and oriented yarns. The DSC examination suggested that the PLLA/PDLA yarns would raise the melt point temperature due to the formation of stereocomplex crystallization in the mixture of PDLA and PLLA. Moreover, the PLLA/PDLA yarns showed 301 MPa tensile strength, which was higher than the other yarns. Furthermore, a 4 cm × 4 cm woven PLLA/PDLA fabric could generate 8.69 V voltage and 90.86 nA current under 5 N forces, which is much higher than the other PLA nanofibrous fabrics. These results indicated that the PLLA/PDLA nanofibrous fabric could be used as a piezoelectric nanogenerator and had potential application in self-powered wearing textile fields.

Funding information: This work was supported by the Postdoctoral Science Foundation of China (2020M671998), the National Natural Science Foundation of China (51703102), Shandong Province Higher Education Youth Innovation

Technology Support Program (2021KJ013), and the State Key Laboratory of Bio-Fibers and Eco-Textiles (Qingdao University) no. ZKT35.

Author contributions: Xin Meng: writing – original draft, writing – review and editing, methodology, formal analysis, investigation; Xiaoyu Jia: formal analysis, conceptualization, writing – review and editing; Yuanzhang Qi: formal analysis, visualization; Dagang Miao: formal analysis, resources; Xu Yan: writing – review and editing, supervision, project administration.

Conflict of interest: The authors state no conflict of interest.

Data availability statement: The raw/processed data required to reproduce these findings are available from the corresponding author on a reasonable request.

References

(1) Hua Y, Dong F. How can new energy vehicles become qualified relays from the perspective of carbon neutralization? Literature review and research prospect based on the CiteSpace knowledge map. Env Sci Pollut Res. 2022;29:55473–91. doi: 10.1007/s11356-022-21096-y.
(2) Sonne C, Xia C, Lam SS. Is engineered wood China's way to carbon neutrality? J Bioresour Bioprod. 2022;7(2):83–4. doi: 10.1016/j.jobab.2022.03.001.
(3) Zheng Q, Li Z, Watanabe M. Production of solid fuels by hydrothermal treatment of wastes of biomass, plastic, and biomass/plastic mixtures: A review. J Bioresour Bioprod. 2022;7(4):221–44. doi: 10.1016/j.jobab.2022.09.004.
(4) Teng X, Zhuang W, Liu F, Chang T, Chiu Y. China's path of carbon neutralization to develop green energy and improve energy efficiency. Renew Energy. 2023;206:397–408. doi: 10.1016/j.renene.2023.01.104.
(5) Qing Y, Liao Y, Liu J, Tian C, Xu H, Wu Y. Research progress of wood-derived energy storage materials. J Eng. 2021;6(5):1–13. doi: 0.13360/j.issn.2096-1359.202012046.
(6) An W, Wang Y, Xiao K, Zhai M, Wang H, Xie Y. Research review of energy storage and conversion materials based on wood cell wall functional modification. J Eng. 2022;7(6):1–12. doi: 10.13360/j.issn.2096-1359.202206011.
(7) Hu Y, Lin L, Zhang Y, Wang Z. Replacing a battery by a nanogenerator with 20 V output. Adv Mater. 2012;24(1):110–14. doi: 10.1002/adma.201103727.
(8) Wen X, Luo J, Xiang K, Zhou W, Zhang C, Chen H. High-performance monoclinic WO3 nanospheres with the novel NH4 + diffusion behaviors for aqueous ammonium-ion batteries. Chem Eng J. 2023;458:141381. doi: 10.1016/j.cej.2023.141381.
(9) Gao J, Shang K, Ding Y, Wen Z. Material and configuration design strategies towards flexible and wearable power supply devices: a review. J Mater Chem A. 2021;9:8950–65. doi: 10.1039/D0TA11260G.
(10) Chen L, Cao S, Huang L, Wu H, Hu H, Liu K, et al. Development of bamboo cellulose preparation and its functionalization. J Eng. 2021;6(4):1–13. doi: 10.13360/j.issn.2096-1359.202104011.
(11) Fan X, Liu B, Ding J, Deng Y, Han X, Hu W, et al. Flexible and Wearable Power Sources for Next-Generation Wearable Electronics. Batteries Supercaps. 2020;3:1262. doi: 10.1002/batt.202000115.
(12) Hu D, Yao M, Fan Y, Ma C, Fan M, Liu M. Strategies to achieve high performance piezoelectric nanogenerators. Nano Energy. 2019;55:288–304. doi: 10.1016/j.nanoen.2018.10.053.
(13) Wang Z, Song J. Piezoelectric nanogenerators based on zinc oxide nanowire arrays. Science. 2006;312:242–46. doi: 10.1126/science.1124005.
(14) Briscoe J, Dunn S. Piezoelectric nanogenerators-a review of nanostructured piezoelectric energy harvesters. Nano Energy. 2015;14:15–29. doi: 10.1016/j.nanoen.2014.11.059.
(15) Wu C, Wang A, Ding W, Guo H, Wang Z. Triboelectric nanogenerator: A foundation of the energy for the New Era. Adv Energy Mater. 2019;9:1802906. doi: 10.1002/aenm.201802906.
(16) Zi Y, Wang J, Wang S, Li S, Wen Z, Guo H, et al. Effective energy storage from a triboelectric nanogenerator. Nat Commun. 2016;7:10987. doi: 10.1038/ncomms10987.
(17) Kwi-Il P, Xu S, Liu Y, Hwang G, Kang L, Wang Z, et al. Piezoelectric BaTiO 3 thin film nanogenerator on plastic substrates. Nano Lett. 2010;10(12):4939–43. doi: 10.1021/nl102959k.
(18) Jiang L, Wang X, Zhang J, Hong H, Du K, Zhang Y, et al. Low temperature calcination induced flexibility in purely inorganic lead zirconate titanate and its application in piezoelectric enhanced adsorption. J Eur Ceram Soc. 2021;41(15):7630–8. doi: 10.1016/j.jeurceramsoc.2021.09.004.
(19) Lu L, Ding W, Liu J, Yang B. Flexible PVDF based piezoelectric nanogenerators. Nano Energy. 2020;78:105251. doi: 10.1016/j.nanoen.2020.105251.
(20) Gong S, Zhang B, Zhang J, Wang Z, Ren K. Biocompatible poly (lactic acid)-based hybrid piezoelectric and electret nanogenerator for electronic skin applications. Adv Funct Mater. 2020;30:1908724. doi: 10.1002/adfm.201908724.
(21) Parangusan H, Ponnamma D, Al-Maadeed MAA. Stretchable electrospun PVDF-HFP/Co-ZnO nanofibers as piezoelectric nanogenerators. Sci Rep. 2018;8(5):153302–4. doi: 10.1038/s41598-017-19082-3.
(22) Hussein AD, Sabry RS. PVDF: ZnO/BaTiO3 as high out-put piezoelectric nanogenerator. Polym Test. 2019;79:106001. doi: 10.1016/j.polymertesting.2019.106001.
(23) Muhterem K, Levent P, Osman Ş. Fabrication and vibrational energy harvesting characterization of flexible piezoelectric nanogenerator (PEN) based on PVDF/PZT. Polym Test. 2020;90:106695. doi: 10.1016/j.polymertesting.2020.106695.
(24) Wu B, Zhu H, Yang Y, Huang J, Liu T, Kuang T, et al. Effect of different proportions of CNTs/Fe3O4 hybrid filler on the morphological, electrical and electromagnetic interference shielding properties of poly(lactic acid) nanocomposites. e-Polymers. 2023;23(1):20230006. doi: 10.1515/epoly-2023-0006.

(25) Ma X, Zhukov S, Seggern H, Sessler GM, Ben DO, Kupnik M, et al. Biodegradable and bioabsorbable polylactic acid ferroelectrets with prominent piezoelectric activity. Adv Electron Mater. 2023;9:2201070. doi: 10.1002/aelm.202201070.
(26) Tran MQ, Hiroshi M, Naogutsu N, Yuki W, Fumio Y, Masao T. Properties of crosslinked polylactides (PLLA & PDLA) by radiation and its biodegradability. Eur Polym J. 2007;43(5):1779–85. doi: 10.1016/j.eurpolymj.2007.03.007.
(27) Sol JL, Anand PA, Kap JK. Piezoelectric properties of electrospun poly(l-lactic acid) nanofiber web. Mater Lett. 2015;148:58–62. doi: 10.1016/j.matlet.2015.02.038.
(28) Tetsuo Y, Kenji I, Komei T, Kyohei N, Yusuke U, Shingo K, et al. Piezoelectricity of poly(L-lactic Acid) composite film with stereocomplex of poly(L-lactide) and poly(D-lactide). Jpn J Appl Phys. 2010;49(9):09MC11. doi: 10.1143/JJAP.49.09MC11.
(29) Yoshiro T. Development of environmentally friendly piezoelectric polymer film actuator having multilayer structure. Jpn J Appl Phys. 2016;55(4S):4. doi: 10.7567/JJAP.55.04EA07.
(30) Zhang J, Wang Y, Tian J, Xu X, Wang W, Ren K. Thermal stability of piezoelectricity in polylactide polymers and related piezoelectric minimotor application. IET Nanodielectr. 2022;5(3–4):132–38. doi: 10.1049/nde2.12038.
(31) Chen GR, Li YZ, Michael B, Chen J. Smart textiles for electricity generation. Chem Rev. 2020;120(8):3668–720. doi: 10.1021/acs.chemrev.9b00821.
(32) Dai Z, Wang N, Yu Y, Lu Y, Jiang L, Zhang D, et al. One-step preparation of a core-spun Cu/P(VDF-TrFE) nanofibrous yarn for wearable smart textile to monitor human movement. ACS Appl Mater Interfaces. 2021;13:44234–42. doi: 10.1021/acsami.1c10366.
(33) Gao H, Minh PT, Wang H, Minko S, Locklin J, Nguyen T, et al. High-performance flexible yarn for wearable piezoelectric nanogenerators. Smart Mater Struct. 2018;27:95018. doi: 10.1088/1361-665x/aad718.
(34) Dai Z, Yan F, Qin M, Yan X. Fabrication of flexible SiO2 nanofibrous yarn via a conjugate electrospinning process. e-Polym. 2020;20:600–5. doi: 10.1515/epoly-2020-0063.
(35) Sun J, Yu H, Zhuang X, Chen X, Jing X. Crystallization behavior of asymmetric PLLA/PDLA blends. J Phys Chem B. 2011;115(12):2864–9. doi: 10.1021/jp111894m.
(36) Wei X, Bao R, Cao Z, Yang W, Xie B, Yang M. Stereocomplex crystallite network in asymmetric PLLA/PDLA blends: Formation, structure, and confining effect on the crystallization rate of homocrystallites. Macromolecules. 2014;47(4):1439–48. doi: 10.1021/ma402653a.